ELSEVIER

Chemical Geology 139 (1997) 21–38

CHEMICAL GEOLOGY
INCLUDING
ISOTOPE GEOSCIENCE

The activities of NiO, CoO and FeO in silicate melts

A. Holzheid *, H. Palme, S. Chakraborty

Universität zu Köln, Institut für Mineralogie und Geochemie, Zülpicher Straße 49b, 50674 Köln, Germany

Accepted 12 July 1996

Abstract

Solubilities of NiO, CoO and FeO in silicate melts have been determined experimentally as a function of temperature, oxidation state and melt composition. The results show that Fe, Ni and Co are dissolved as divalent cations in silicate melts at oxygen fugacities varying from IW +1.5 to IW −3. The well defined valence state of these elements in the melt allows the calculation of activity coefficients. The activity coefficients of FeO, NiO and CoO in the silicate melt, calculated by assuming oxides as melt components, were found to be independent of oxygen fugacity and of temperature within a temperature range of 1300°C to 1600°C. Earlier reports on temperature-dependent NiO activity coefficients were based on a standard state for NiO in the melt of solid NiO. When the more appropriate liquid standard state is used, the temperature dependence disappears. The activity coefficients were not affected by variations in FeO (from 0 to 12 wt.%) and MgO (from 4 to 30 wt.%) contents, except for a small increase of γ_{CoO} and $\gamma_{\cdot\cdot FeO\cdot\cdot}$ at MgO-contents above 20 wt.%. The average activity coefficients obtained are $\gamma_{NiO} = 2.70 \pm 0.52$ (77 experiments), $\gamma_{CoO} = 1.51 \pm 0.28$ (76 exp.) and $\gamma_{\cdot\cdot FeO\cdot\cdot} = 1.70 \pm 0.22$ (57 exp.) relative to the respective pure liquid oxide standard states and simple oxide mole fractions.

From the activities of NiO and CoO and additional thermodynamic data a distribution coefficient $K_D^{Ni/Co}$ (Ni/Co-olivine/Ni/Co-melt) is calculated. The $K_D^{Ni/Co}$ is slightly temperature-dependent, increasing from 1.13 ± 0.28 at 1100°C to 1.34 ± 0.33 at 1600°C.

The difference between the activity coefficients of NiO and CoO in silicate liquids is responsible for the preferred partitioning of Ni into olivine, i.e., the larger $D^{Ni}_{olivine/melt}$ ($NiO_{olivine}/NiO_{melt}$) compared to $D^{Co}_{olivine/melt}$ is, contrary to general belief, not the result of preferred acceptance of Ni into the olivine structure, but of stronger rejection of NiO compared to CoO from the melt. Simple considerations based on crystal field stabilization energy (CFSE) can rationalize but not explain quantitatively the high NiO activity coefficient in silicate melts compared to CoO and FeO and the nearly ideal mixing of Ni-olivine and Co-olivine with Mg-olivine. It is suggested that the high degree of preference of Ni for octahedral coordination rather than the tetrahedral sites at high temperatures in the melt is responsible for the unusual behaviour of NiO.

Keywords: metal-oxide; olivine fractionation; activity coefficient; silicate melt

* Corresponding author. Present address: MIT, Department of Earth and Planet Science, Cambridge, MA 02133-4307, USA. FAX: 617 253 7102; E-mail: holzheid@mit.edu.

0009-2541/97/$17.00
PII S0009-2541(97)00030-2

1. Introduction

During the last few years a large number of experiments have been performed in this laboratory to determine metal/silicate partition coefficients of Ni, Co and several other metals in order to constrain models of core formation in the Earth (e.g., Holzheid et al., 1994; Borisov et al., 1994; O'Neill et al., 1995; Holzheid and Palme, 1996a,b). These experiments were done at a wide range of oxygen fugacities and at temperatures from 1300°C to 1600°C (at 1 atm) and, to a limited extent, at high pressures, up to 20 GPa.

In earlier work on metal/silicate partition experiments (e.g., Schmitt et al., 1989) the Fe-metal phase was doped with a trace element, for example Ni, and then equilibrated with silicate liquids. In the more recent experiments silicates were equilibrated with pure metals, e.g. Ni. This is equivalent to the determination of solubilities of the given metal. From solubilities, metal/silicate partition coefficients may be calculated using activity–composition relationships in metallic alloy phases (see Borisov et al., 1994). This new procedure is in many cases superior to the earlier determinations because the concentrations of metals dissolved in the silicate are higher and can be determined more accurately.

These experiments have led to a large database on solubilities of Ni, Co, Fe, Mo, W, Pd and Ir in silicate melts (Holzheid et al., 1994; Borisov et al., 1994; Dingwell et al., 1994; Borisov and Palme, 1995; O'Neill et al., 1995; Holzheid and Palme, 1996a; Ertel et al., 1996b). From solubilities, activities and activity coefficients of oxides in silicate melts can be calculated if the formal valence of the metal in the silicate melt is known and if an appropriate thermodynamic model of the melt is chosen. Activity coefficients calculated from solubilities provide direct information on the interaction of the metal-oxide with the other components of the melt and thus allow conclusions to be drawn regarding the structure of the melt. In addition, the knowledge of activity coefficients is important in predicting the behaviour of trace elements during igneous fractionation. In this paper we will focus on the activities of NiO, CoO and FeO in silicate liquids and study the implications of the new data for olivine crystallization and finally make some attempts to understand the activity coefficients within the framework of structural models of silicate melts.

2. Solubilities of NiO, CoO and FeO in silicate melts

2.1. Summary of earlier results

The main results of recent studies on Ni and Co metal-silicate partition coefficients may be summarized as follows:

(a) Ni and Co are, over a wide range of oxygen fugacities, dissolved as divalent cations in silicate melts (Holzheid et al., 1994; Dingwell et al., 1994). Earlier claims that metallic Ni and Co are important species at oxygen fugacities below IW were not confirmed (Colson, 1992; Ehlers et al., 1992). NiO and CoO are the most abundant stable Ni- and Co-species in silicate melts at oxygen fugacities ranging from pure oxygen to oxygen fugacities as low as IW −3.

(b) The solubility of Co shows little dependence on temperature (from 1300°C to 1600°C), while Ni-solubilities increase significantly with increasing temperature and increasing pressure (Holzheid and Palme, 1996a; Righter et al., 1996 and literature cited therein). This leads to decreasing Ni/Co ratios in silicate liquids equilibrated with metal of fixed Ni/Co at different temperatures.

(c) Ni and Co solubilities do not depend on the FeO-content of the silicate melt with FeO-contents of up to 12 wt.%. There is also no apparent dependence of NiO and CoO solubilities on the MgO-content of the silicate melt, at least up to 20 wt.% MgO. More data on the MgO-dependence were obtained in this study (see below).

Silicates with the composition of the anorthite–diopside eutectic (AD) and a komatiitic basalt (BK)

Table 1
Silicate starting compositions (electron microprobe analysis)

wt.%	AD (anorth.–diopside)	BK (komatiitic basalt)
SiO_2	50.9	49.1
CaO	24.9	19.2
MgO	10.4	10.6
Al_2O_3	13.8	14.1
FeO	0.0	7.0

Table 2
Mole fraction and activity coefficients (γ) of metal oxides

Run	T (K)	log f_{O_2}	X_{CoO}	X_{FeO}	X_{NiO}	X_{FeO}	γ_{CoO}	γ_{NiO}	$\gamma_{"FeO"}$
(a) Experiments in the AD-system (initially FeO-free), $T = 1400$°C, f_{O_2} variable									
Silicate: anorthite–diopside; metal: Co, Ni									
AD 60	1672	−8.08	10.1		0.71		1.76	3.75	
AD 25	1678	−8.47	5.37		0.37		2.02	4.36	
AD 13	1676	−9.43	2.62		0.17		1.40	3.18	
AD 12	1677	−9.64	2.17		0.16		1.31	2.61	
AD 7	1681	−9.99	1.26		0.085		1.47	3.25	
AD 10	1677	−10.31	0.93		0.068		1.42	2.90	
AD 6	1677	−10.60	0.62		0.044		1.53	3.21	
AD 1	1679	−10.63	0.62		0.042		1.45	3.24	
AD 8	1682	−10.80	0.47		0.035		1.53	3.05	
AD 11	1678	−10.92	0.42		0.034		1.53	2.84	
AD 5	1677	−11.10	0.34		0.028		1.57	2.81	
AD 9	1679	−11.29	0.27		0.023		1.55	2.77	
AD 14	1677	−11.42	0.24		0.016		1.54	3.39	
AD 14**	1677	−11.42	0.24		0.018		1.53	3.05	
AD 2	1680	−11.62	0.18		0.016		1.55	2.70	
AD 3	1680	−11.72	0.15		0.017		1.66	2.29	
AD 17	1676	−12.21	0.084		0.010		1.76	2.22	
AD 26	1678	−12.32	0.069		0.0086		1.86	2.24	
AD 16	1678	−12.47	0.059		0.0087		1.84	1.87	
AD 15	1676	−12.55			0.0061			2.45	
Silicate: anorthite–diopside; metal: FeNiCo-alloy									
AD 10	1677	−10.31	0.25		0.027	5.56	1.51	3.82	1.62
AD 6	1677	−10.60	0.13		0.025	8.77	1.62	1.73	1.64
AD 1	1679	−10.63	0.12		0.013	8.13	1.57	3.03	1.74
AD 8	1682	−10.80	0.095		0.013	6.66	1.69	2.69	1.61
AD 5	1677	−11.10	0.085		0.0085	4.61	1.51	3.25	1.56
AD 9	1679	−11.29	0.065		0.0071	4.16	1.46	2.46	1.63
AD 2	1680	−11.62	0.044		0.0066	2.60	1.51	2.20	1.52
AD 3	1680	−11.72	0.037		0.0043	2.66	1.49	2.93	1.39
(b) Experiments in the BK-system, $T = 1400$°C, f_{O_2} variable									
Silicate: komatiitic basalt; metal: Co, Ni									
BK 60 a	1672	−8.08	10.8	3.86			1.25		2.27
BK 60 b	1672	−8.08			0.85	4.72		3.03	1.78
BK 59 a	1672	−8.53	6.12	4.37			1.30		2.47
BK 59 b	1672	−8.53			0.62	4.07		1.70	1.78
BK 58 a	1675	−9.05	3.38	4.23			1.26		1.82
BK 58 b	1675	−9.05			0.37	2.69		2.15	1.72
BK 57 a	1673	−9.58	1.89	3.69			1.21		1.69
BK 57 b	1673	−9.58			0.19	1.80		2.33	1.65
BK 56 a	1674	−10.06	0.99	3.01			1.29		1.93
BK 56 b	1674	−10.06			0.087	1.37		2.80	1.73
BK 54 a	1674	−10.61	0.68	1.74			1.01		1.49
BK 54 b	1674	−10.61			0.042	0.91		3.05	1.70
BK 55 a	1675	−11.05	0.34	1.11			1.24		1.12
BK 55 b	1675	−11.05			0.025	0.65		3.01	1.59
BK 49 a	1673	−11.57	0.20	1.08			1.12		1.57
BK 49 b	1673	−11.57			0.015	0.63		2.54	1.48
BK 53 a	1675	−11.89	0.43	0.34			0.95		1.59
BK 53 b	1675	−11.89			0.012	0.30		2.24	1.71

Table 2 (continued)

Run	T (K)	log f_{O_2}	X_{CoO}	X_{FeO}	X_{NiO}	X_{FeO}	γ_{CoO}	γ_{NiO}	γ_{FeO}
Silicate: komatiitic basalt; metal: FeCo, FeNi alloys									
BK 59 a	1672	−8.58	5.15	4.24			1.46		2.00
BK 59 b	1672	−8.58			0.47	5.88		3.00	1.19
BK 58 a	1675	−9.05	2.35	3.42			1.78		2.45
BK 58 b	1675	−9.05			0.26	5.21		2.93	1.85
BK 57 a	1673	−9.58	1.69	3.64			1.36		2.06
BK 57 b	1673	−9.58			0.14	4.42		2.87	1.77
BK 56 a	1674	−10.06	1.06	3.79			1.21		1.89
BK 56 b	1674	−10.06			0.075	2.93		2.94	1.76
BK 54 a	1674	−10.61	0.54	3.75			1.17		1.75
BK 54 b	1674	−10.61			0.037	4.17		2.46	1.56
BK 55 a	1675	−11.05	0.26	3.66			1.30		1.81
BK 55 b	1675	−11.05			0.016	3.07		3.04	1.68
BK 51 a	1672	−11.58	0.093	5.01			1.45		1.40
BK 51 b	1672	−11.58			0.0052	4.46		2.46	1.52
BK 53 a	1675	−11.89	0.0072	4.35			1.43		1.81
BK 53 b	1675	−11.89			0.015	4.95		2.07	1.59
(c) Experiments at variable temperatures and oxygen fugacities									
Silicate: anorthite–diopside; metal: Co, Ni									
AD 50	1578	−12.54	0.15		0.011		1.51	3.04	
AD 18	1622	−11.64	0.32		0.024		1.37	2.69	
AD 24	1623	−10.32	1.51		0.100		1.32	2.98	
AD 42	1623	−12.07	0.22		0.016		1.22	2.56	
AD 41	1673	−11.58	0.23		0.022		1.38	2.18	
AD 10	1677	−10.31	0.93		0.068		1.42	2.90	
AD 2	1680	−11.62	0.18		0.016		1.55	2.70	
AD 23	1711	−10.31	0.67		0.062		1.51	2.48	
AD 19	1712	−11.70	0.11		0.015		1.92	2.08	
AD 40	1713	−11.21	0.24		0.023		1.49	2.35	
AD 36	1759	−10.84	0.23		0.021		1.74	2.83	
AD 30	1775	−10.31	0.33		0.029		1.97	3.43	
AD 31	1775	−10.69	0.24		0.018		1.76	3.47	
AD 35	1778	−10.67	0.23		0.024		1.83	2.66	
AD 39	1793	−10.51			0.028			2.42	
AD 38	1794	−10.32	0.38				1.51		
AD 37	1796	−10.33	0.36		0.031		1.54	2.69	
AD 32	1824	−10.33	0.25		0.021		1.81	3.28	
AD 33	1825	−10.26	0.25		0.025		1.96	3.01	
AD 29	1872	−10.27	0.19		0.034		1.96	1.65	
AD 34	1873	−9.84	0.33		0.030		1.82	2.98	
Silicate: anorthite–diopside; metal: FeNiCo-alloy									
AD 50	1578	−12.54	0.030		0.0046	2.99	1.55	2.16	1.58
AD 43	1623	−12.03	0.036		0.0046	2.67	1.44	2.72	2.02
AD 49	1673	−11.57	0.056		0.0056	3.05	1.24	2.76	1.58
AD 46	1711	−11.29	0.042		0.0066	3.19	1.47	2.06	1.64
AD 47	1755	−10.79	0.037		0.0055	3.05	1.76	2.81	2.00
AD 48	1780	−10.59	0.044		0.0067	3.48	1.61	2.49	1.70
AD 44	1795	−10.46	0.044		0.0063	3.27	1.73	2.83	1.78
AD 52	1826	−10.23	0.045		0.0080	3.36	1.75	2.34	1.73
AD 45	1872	−9.73	0.049		0.0085	3.34	2.16	2.96	2.02

Table 2 (continued)

Run	T (K)	log f_{O_2}	X_{CoO}	X_{FeO}	X_{NiO}	X_{FeO}	γ_{CoO}	γ_{NiO}	$\gamma_{"FeO"}$
Silicate: komatiitic basalt; metal: Co, Ni									
BK 50 a	1578	−12.54	0.34	0.91			0.47		1.39
BK 50 b	1578	−12.54			0.024	0.25		1.27	1.68
BK 49 a	1673	−11.57	0.20	1.08			1.12		1.57
BK 49 b	1673	−11.57			0.015	0.63		2.54	1.48
BK 46 a	1711	−11.19	0.36	0.83			0.73		1.53
BK 46 b	1711	−11.19			0.018	0.45		2.63	1.54

were used as starting materials. Bulk compositions are listed in Table 1. In addition, silicates with variable MgO-compositions were produced by adding or removing MgO from the AD- and BK-composition. Run durations as dictated by reversal experiments in Holzheid et al. (1994) were chosen such that equilibrium is attained. A summary of the results is listed in Table 2. This table contains the sample number, temperature, oxygen fugacity and the mole percent of NiO, CoO, and FeO, calculated on the basis of a simple decomposition of the liquid into oxides. The last columns contain the calculated activity coefficients (see below). Further experimental details are given in Holzheid et al. (1994) and Holzheid and Palme (1996a). In Table 2(a) the results of experiments in the AD-system (initially FeO-free) at a temperature of 1400°C and with variable oxygen fugacities are compiled. Table 2(b) contains results with FeO-containing starting materials at constant temperature (1400°C) and variable oxygen fugacities. Results of experiments at variable temperatures are reported in Table 2(c). No effect of addition of FeO (up to 12 wt.% FeO) on the behaviour of NiO and CoO in silicate liquid were found (Holzheid and Palme, 1996a). Experiments with FeO-containing silicates were made with FeNi, FeCo or FeNiCo metal alloys. The results are recalculated to equilibria with 100% pure metals by using relevant alloy activity coefficients from the literature as described by Holzheid and Palme (1996a). Alloy experiments are thus equivalent to equilibrium experiments with pure metals, except for additional uncertainties arising from the determination of alloy compositions after the experiment and insufficient knowledge of alloy activity coefficients.

2.2. New experimental results

Additional experiments were made to extend the range of MgO-contents in the silicate liquids. These experiments were done in the same way as those described before. The major element composition of the silicates were determined with the electron microprobe while Ni and Co concentrations were obtained by instrumental neutron activation analyses. To check for the homogeneity of the Ni and Co contents samples were, after the first counting, disintegrated into smaller pieces which were then individually counted. The analytical errors in the Ni and Co determinations are below 10%. Results of the new analyses are given in Table 3. The MgO-content in these experiments varies from 5 to 30.5 wt.%.

3. Calculation of activity coefficients

The calculation of activity coefficients will be discussed for Ni. The treatment of Co and Fe is completely analogous. The oxidation of metallic Ni is given by:

$$Ni(s) + 1/2 \cdot O_2(g) = NiO(s) \quad (1)$$

where s and g indicate solid and gaseous states, respectively.

Equilibrium between pure metallic Ni and NiO dissolved in a solid silicate phase is described by:

$$\log K^{Ni-NiO(s)} = -1/2 \cdot \log f_{O_2} + \log X_{NiO} + \log \gamma_{NiO} \quad (2)$$

where $K^{Ni\text{-}NiO(s)}$ is the equilibrium constant of reaction (1), X_{NiO} the oxygen fugacity imposed on the

Table 3
Equilibration of metal and silicate melts with variable MgO-content: T = constant, f_{O_2} = constant, X_{MgO} = variable

(a) Silicate: anorthite–diopside; metal: Co

Run#	T (K)	Duration (h)	log f_{O_2}	CoO (wt.%)	s.d. (%)	MgO (wt.%)	s.d. (%)	γ_{CoO}
V 69	1673	50	−9.63	2.03	5	6.97	1	1.72
AD 12	1677	48	−9.64	2.80	5	10.1	1	1.31
V 70	1670	48	−9.93	1.85	5	10.8	1	1.46
V 64	1675	49	−9.79	2.13	5	17.4	1	1.49
V 66	1671	74.3	−9.64	1.06	5	18.2	1	3.66
V 70	1670	48	−9.93	1.63	5	19.3	1	1.77
V 66	1671	74.3	−9.64	0.76	5	22.0	7	4.93
V 65	1671	48.5	−9.66	0.62	5	27.3	9	6.22

Silicate: anorthite–diopside; metal: Ni

Run#	T (K)	Duration (h)	log f_{O_2}	NiO (wt.%)	s.d. (%)	MgO (wt.%)	s.d. (%)	γ_{NiO}
V 69	1673	50	−9.64	0.17	6	7.22	1	3.06
V 69	1673	50	−9.64	0.21	5	8.94	1	2.60
AD 12	1677	48	−9.64	0.26	5	10.4	1	2.61
V 70	1670	48	−9.93	0.13	5	11.1	1	3.07
V 70	1670	48	−9.93	0.16	6	13.8	1	2.59
V 64	1675	49	−9.79	0.15	5	17.6	1	3.21
V 66	1671	74.3	−9.64	0.20	10	18.2	1	2.84
V 70	1670	48	−9.93	0.13	9	18.2	1	3.30
V 66	1671	74.3	−9.64	0.18	5	22.2	7	3.20
V 65	1671	48.5	−9.66	0.17	5	27.5	9	3.39

(b) Silicate: anorthite–diopside; metal: FeNiCo-alloy

Run#	T (K)	Duration (h)	log f_{O_2}	silicate								metal						γ_{CoO}	γ_{NiO}	γ_{FeO}
				CoO (wt.%)	s.d. %	NiO (wt.%)	s.d. %	FeO (wt.%)	s.d. %	MgO (wt.%)	s.d. %	Co (wt.%)	s.d. %	Ni (wt.%)	s.d. %	Fe (wt.%)	s.d. %			
V 69	1673	50	−9.63	0.465	5	0.0518	18	26.0	5	4.87	1	20.1	1	37.7	1	41.9	1	1.65	3.68	1.72
V 69	1673	50	−9.63	0.531	5	0.0502	15	20.8	5	6.83	1	22.6	3	41.2	2	36.0	1	1.75	4.35	1.83
AD 10	1677	50	−10.31	0.334	5	0.0360	7	7.15	5	9.73	1	18.7	5	48.2	5	22.1	14	1.51	3.82	1.62
V 64	1677	49	−9.79	0.280	5	0.0385	19	15.5	5	15.3	1	20.3	2	39.2	1	39.1	1	2.68	4.87	2.47
V 68	1667	49	−9.70	0.286	5	0.0457	15	15.8	5	15.8	1	19.4	2	35.6	1	44.3	1	2.89	4.34	3.44
V 66	1671	74.3	−9.64	0.259	5	0.0367	15	10.6	5	20.0	5	21.0	2	38.7	1	39.8	1	3.53	5.99	4.41
V 66	1671	74.3	−9.64	0.313	5	0.0689	6	9.56	5	25.0	7	20.9	1	38.4	1	40.0	1	3.06	3.33	5.22

(c) Silicate: komatiitic basalt; metal: Co

Run #	IT (K)	Duration (h)	log f_{O_2}	silicate						metal						γ_{CoO}	$\gamma_{"FeO"}$
				CoO (wt.%)	s.d. (%)		FeO (wt.%)	s.d. (%)	MgO (wt.%)	s.d. (%)	Co (wt.%)	s.d. (%)		Fe (wt.%)	s.d. (%)		
BK 57	1673	66	−9.58	2.40	5		4.48	5	10.6	1	91.3	1		6.38	1	1.21	2.33
V 68	1667	49	−9.70	1.78	5		2.65	6	17.7	6	91.4	2		8.06	5	2.08	3.44
V 64	1675	49	−9.79	2.13	5		2.20	10	17.9	1	90.8	1		7.12	1	1.48	3.24
V 68	1667	49	−9.79	1.86	5		1.94	10	30.5	1	92.8	1		7.28	1	1.89	4.01

(d) Silicate: komatiitic basalt; metal: Ni

Run #	T (K)	Duration (h)	log f_{O_2}	silicate						metal						γ_{NiO}	$\gamma_{"FeO"}$
				NiO (wt.%)	s.d. (%)		FeO (wt.%)	s.d. (%)	MgO (wt.%)	s.d. (%)	Ni (wt.%)	s.d. (%)		Fe (wt.%)	s.d. (%)		
BK 57	1673	66	−9.58	0.219	5		2.01	12	11.1	1	91.1	1		5.65	6	2.33	1.65
V 68	1667	49	−9.70	0.167	5		2.19	5	17.4	6	89.5	1		9.50	6	2.84	2.79
V 64	1675	49	−9.79	0.130	10		1.72	5	17.5	1	90.5	1		8.52	3	3.15	2.59
V 67	1667	75.3	−9.79	0.171	5		0.975	5	30.0	1	92.5	1		6.84	3	2.74	3.99

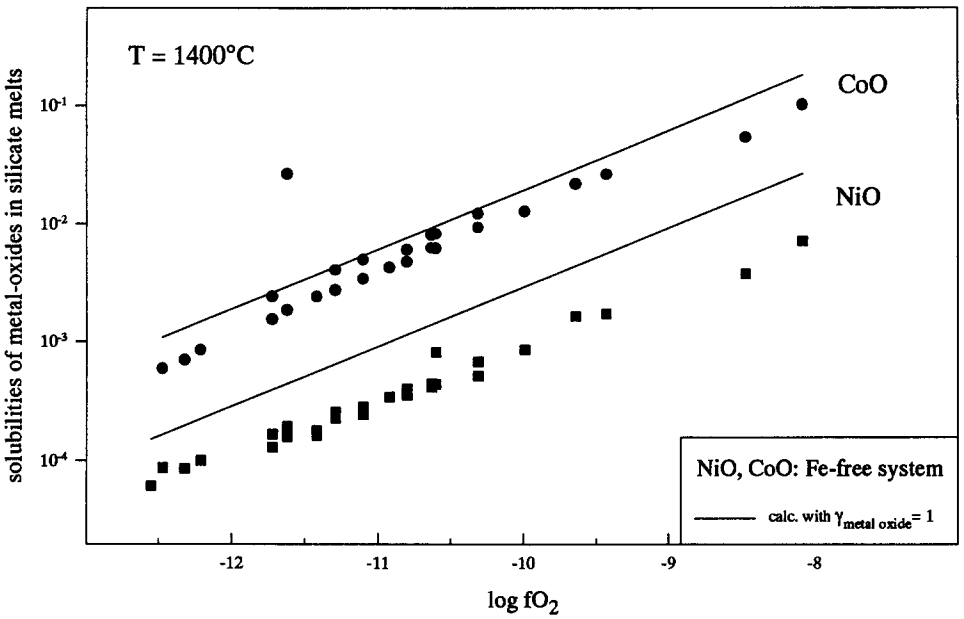

Fig. 1. Solubilities of Co and Ni in a melt of anorthite–diopside eutectic composition as function of oxygen fugacity at a temperature of 1400°C (see Table 1). The lines parallel to the data points are based on calculations assuming 2^+ metal ions and ideal solid solution of NiO and CoO in the silicate liquid, i.e., $\gamma_{NiO} = \gamma_{CoO} = 1$.

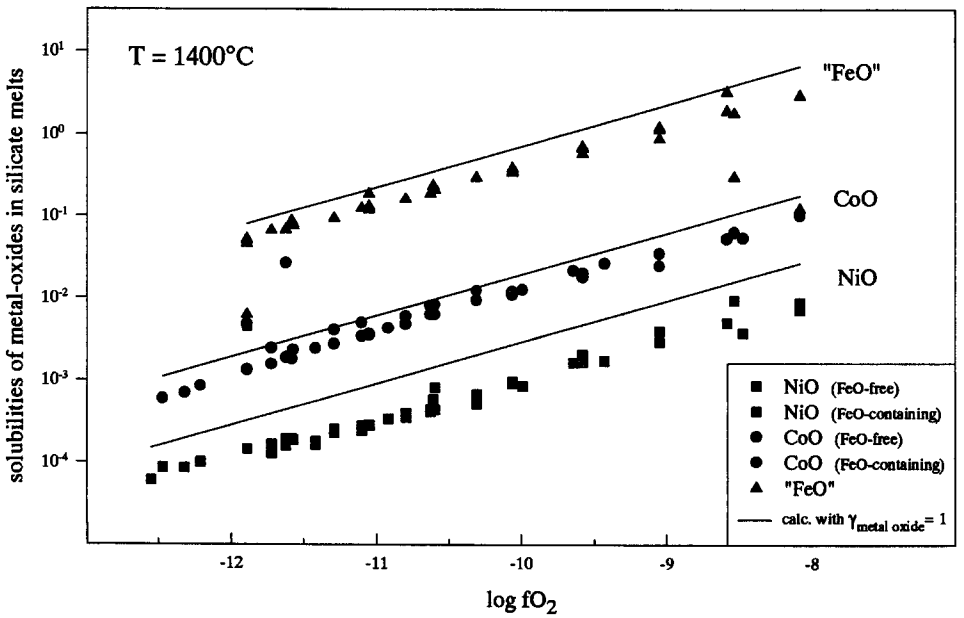

Fig. 2. Similar plot as Fig. 1, except that FeO is included. Data for FeO-free and FeO-containing systems are distinguished by different symbols. Apparently, there is no difference between the two systems. Some of the data points were obtained from experiments with alloys. In these cases measured NiO and CoO concentrations were recalculated to pure metal solubilities by plotting, e.g., $X_{NiO}/X_{Ni} \cdot \gamma_{Ni}$ (see Holzheid and Palme, 1996a for details). The distance between the lines indicating ideal solid solutions and the actual data points is proportional to the log of the respective activity coefficients.

system during equilibration, f_{O_2} the mole fraction of NiO in the silicate and γ_{NiO} the corresponding activity coefficient of NiO. Thus, if f_{O_2} is known and with appropriate decomposition of the silicate the corresponding activity coefficient can be calculated.

So far we have assumed equilibrium of metallic Ni and solid NiO(s). As we are interested in the solubilities of NiO in liquid silicates it is more appropriate to use liquid NiO as standard state, even at temperatures below the melting point of NiO at 1955°C. Addition of

$$NiO(s) = NiO(l) \quad (3)$$

to Eq. (1) yields the final expression used for calculating the activity coefficients of NiO in silicate melt relative to pure liquid oxide at 1 atm, T standard state as:

$$\log \gamma_{NiO} = \log K^{Ni-NiO(l)} - \log X_{NiO} + 1/2 \cdot \log f_{O_2} \quad (4)$$

In Fig. 1 we have plotted the experimentally determined Ni-solubilities for silicate liquids with anorthite–diopside eutectic compositions at a temperature of 1400°C (see Table 2). The data form a remarkably straight line with a slope of 0.48 ± 0.01 reflecting the 2^+ valence of NiO in the silicate melt. A similar correlation with a slope of 0.49 ± 0.01 was obtained for CoO. In Fig. 1 parallel lines to the data with a slope of 0.5 are drawn indicating calculated NiO (and CoO) solubilities by assuming ideal solution of NiO and CoO in the melt, i.e., using Eq. (4) and assuming $\gamma_{NiO} = \gamma_{CoO} = 1$. The difference between the line assuming ideal mixing and the actual data array is given by $\log \gamma_{NiO}$ and $\log \gamma_{CoO}$, respectively. In Fig. 2 similar plots are shown for Ni, Co and Fe for all experiments at 1400°C, including experiments with FeO-containing and FeO-free systems. This figure clearly shows that there is no difference in NiO and CoO solubilities between FeO-free and FeO-containing silicates.

Figs. 1 and 2 demonstrate that Ni, Co and Fe are, within geologically relevant oxygen fugacities, in a 2^+ state in silicate melts. This is an essential prerequisite for the calculation of meaningful activity coefficients. The factor 0.5 in Eq. (4) is a reflection of the 2^+ state of Ni, Co and Fe. Activity coefficients for NiO, CoO and FeO (see below) in silicate melts were calculated according to this equation. In calculating the free energy of formation of NiO(l) and CoO(l) the entropy of fusion ΔS_m and the enthalpy of fusion ΔH_m as measured at the respective melting points were assumed to be independent of temperature:

$$\Delta G(3) = \Delta H_m - T \cdot \Delta S_m \quad (5)$$

The values for ΔH_m and ΔS_m of CoO and NiO at temperatures above the temperatures of fusion listed in Barin (1989) are constant within uncertainties of the data.

With these data the equilibrium constant of the reaction

$$Ni(s) + \frac{1}{2} \cdot O_2(g) = NiO(l) \quad (6)$$

and corresponding reactions for Co and Fe were calculated from the free energies of formation, using thermodynamic data from O'Neill and Pownceby (1993) and Barin (1989). The results for the ΔG of reaction (6) and corresponding reactions for Co and Fe are:

NiO(l):

$$\Delta G(NiO_l)\ [J/mol] = -185092 + 99.844 \cdot T - 4.898 \cdot T \cdot \ln T \quad (7)$$

CoO(l):

$$\Delta G(CoO_l)\ [J/mol] = -187746 + 91.371 \cdot T - 5.672 \cdot T \cdot \ln T \quad (8)$$

Table 4
Summary of activity coefficients γ of metal oxides

	γ_{CoO}	s.d.	γ_{NiO}	s.d.	$\gamma_{\cdot\cdot FeO\cdot\cdot}$	s.d.
T = const., f_{O_2} = variable						
system A	1.59	0.17	2.91	0.56		
system B	1.54	0.08	2.76	0.61	1.59	0.10
system C	1.18	0.12	2.54	0.45	1.68	0.22
system D	1.39	0.18	2.81	0.23	1.77	0.28
all data	1.46	0.22	2.79	0.53	1.71	0.25
T = variable, f_{O_2} = variable						
system A	1.64	0.24	2.70	0.45		
system B	1.63	0.25	2.57	0.30	1.78	0.17
system C	0.77	0.27	1.64	0.39	1.78	0.48
all data	1.55	0.35	2.61	0.46	1.68	0.19
Average of all data	1.51	0.28	2.70	0.52	1.70	0.22
Std. dev. of the mean		0.03		0.06		0.03

"FeO"(l):

$$\Delta G(\text{"FeO"}_l)\ [\text{J/mol}] = -244118 + 115.559 \cdot T - 8.474 \cdot T \cdot \ln T \quad (9)$$

From these data activity coefficients were calculated according to Eq. (4) and using the mole fractions given in Table 2. The calculated activity coefficients are listed in Table 2. Average activity coefficients for the different systems and global averages are given in Table 4. Using stoichiometric FeO as standard state instead of wüstite yields slightly higher activity coefficients. The activity coefficient ratio $\gamma_{FeO}/\gamma_{\text{"FeO"}}$ (activity coefficient relative to stoichiometric FeO divided by the activity coefficient relative to wüstite) can be calculated from thermodynamic data as the ratio of equilibrium constants for the formation of stoichiometric FeO and wüstite, ignoring small differences in mole fraction between FeO and wüstite. Using thermodynamic data by Barin (1989) this activity coefficient ratio ($\gamma_{FeO}/\gamma_{\text{"FeO"}}$) is calculated as of 2.02 at 1300°C and 1.66 at 1600°C.

4. Discussion

4.1. Activity coefficients

The NiO and CoO activity coefficients calculated here are lower than those listed in Holzheid and Palme (1996a) and in other papers (Campbell et al., 1979; Doyle and Naldrett, 1987; Snyder and Carmichael, 1992). The reason is that in the earlier papers NiO(s) and CoO(s) were used as standard states for the calculation of the activity coefficients of NiO and CoO, except for the paper by Leeman and Lindstrom (1978) who made an attempt to consider NiO(l). The difference between the solid and liquid standard state is shown in Fig. 3, where the free energies of formation of NiO(s) and NiO(l) are compared. The difference between the two standard states increases with increasing distance from the melting temperature. Therefore, the distribution is at any given temperature more pronounced for NiO with a melting temperature of 2228 K than for CoO with a temperature of fusion of 2078 K. For wüstite

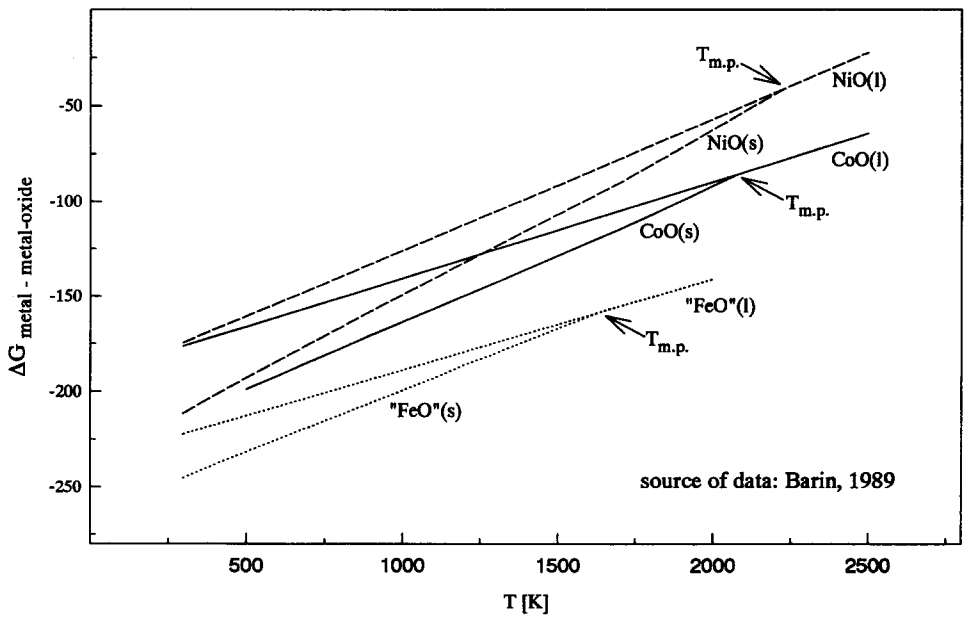

Fig. 3. The free energy of formation of solid MO(s) and liquid MO(l), (M = Ni, Co, Fe). The difference between the two standard states increases with increasing distance from the melting temperature. For example, at 1500 K the difference is largest for NiO, smaller for CoO and negligible for "FeO" (wüstite). The difference between the two standard states produces a corresponding difference in calculated activity coefficients.

the difference is very small, at least within the temperature range of 1400°C to 1600°C (Fig. 3).

Figs. 4 and 5 show the calculated activity coefficients relative to the liquid and solid reference states as function of oxygen fugacity (Fig. 4) and temperature (Fig. 5). For FeO we have chosen an "FeO"–wüstite(l) standard state. For comparison, activity coefficients calculated relative to stoichiometric FeO(l) are plotted as open diamonds in Fig. 4. The activity coefficients using a stoichiometric FeO(l) standard state are higher by a factor of 1.94 (at 1400°C) relative to the activity coefficients based on wüstite(l). In Fig. 5 there is a slight tendency for CoO-activity coefficients to decrease with increasing temperature when using the liquid standard state. Calculations with the solid standard state produce a small temperature increase of the activity coefficients. An even stronger increase with temperature of the NiO-activity coefficient is observed when using the solid NiO standard state. However, when using the correct liquid standard state the temperature dependence of the NiO activity coefficients disappears. This is a consequence of the decreasing difference between the solid and liquid standard states with increasing temperature as shown in Fig. 3. Thus, there is essentially no statistically resolvable temperature dependence of the activity coefficients of FeO, CoO and NiO within the temperature range of 1300°C and 1600°C. Therefore, averages of all activity coefficients were calculated for runs with about 10% MgO (Table 4). The average γ_{NiO} is 2.70 ± 0.52 or ± 0.063 if the standard deviation of the mean is calculated. This is nearly two times more than the average γ_{CoO} of 1.51 ± 0.28 (± 0.03 for the standard deviation of the mean) and the average $\gamma_{\text{"FeO"}}$ with 1.70 ± 0.22 (± 0.03). The average CoO activity coefficient is slightly lower than that of FeO, statistically significant if the standard deviation of the mean is considered. However, it is not clear if there are minor differences in the activity coefficients depend-

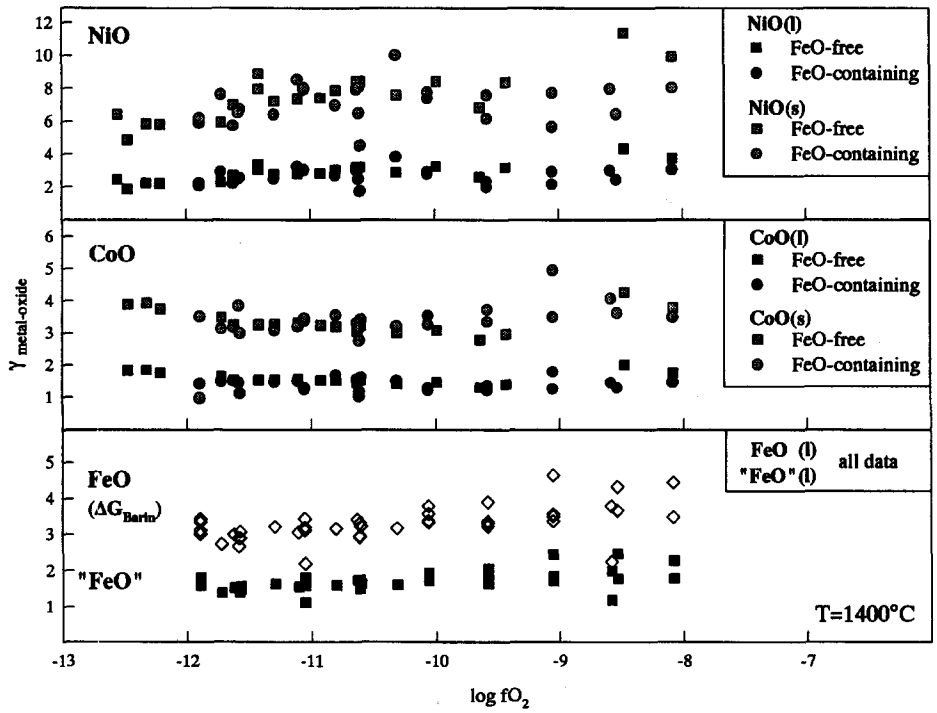

Fig. 4. Summary for calculated activity coefficients as function of oxygen fugacity. The full symbols indicate activity coefficients calculated relative to the liquid standard states. The grey-shaded squares and circles symbolize activity coefficients calculated relative to the solid standard states. Open diamonds symbolize activity coefficients of FeO calculated with ΔG (FeO_l)-values instead of ΔG ("FeO"$_l$ = wüstite)-values. Most data in the literature were calculated with the solid standard state of the metal-oxides.

ing on composition which are, at present, statistically unresolvable.

The new experiments, with variable MgO-contents (Table 3), show some dependence of the activity coefficients of "FeO" and CoO on composition (Fig. 6). The first four experiments of Table 3(a) in the AD-system (with variable MgO) have CoO activity coefficients within the range of the global average (Table 4). Experiments with high MgO-contents above 20 wt.% show a distinct increase in γ_{CoO}. A less pronounced increase is found for γ_{NiO}, from 2.7 to 3.4. The same basic trends are also seen in the other experiments (Table 3(b–d)). It should be emphasized that experiments with alloys or with komatiitic basalt composition ±MgO have higher uncertainties due to the uncertainties involved with alloys where metal activity coefficients were used to calculate the equilibrium with pure metals.

It is also important to point out that all compositions used in these experiments have very similar SiO_2, CaO and Al_2O_3 contents, except for some variation caused by addition or removal of MgO. Ertel et al. (1996a) noticed some increase in the solubility of NiO in AD-compositions with increasing CaO-contents. Because of the uniform CaO-contents in our samples we are unable to see this effect in the present experiments.

In summary, we have shown that activity coefficients of FeO, CoO, and NiO in silicate melts with anorthite–diopside eutectic composition modified by addition of FeO and addition and removal of MgO are constant within about 20%. The activity coefficients do not depend on oxygen fugacity (IW +1.5 to −3), are independent of temperature (1300°C to 1600°C) and do not depend on FeO and MgO contents of the liquid with MgO up to about 20%. At higher MgO-contents FeO and CoO activity coefficients increase with MgO.

4.2. Comparison with literature data

Roeder (1974) obtained FeO-activity coefficients (relative to a liquid wüstite standard state) in basaltic

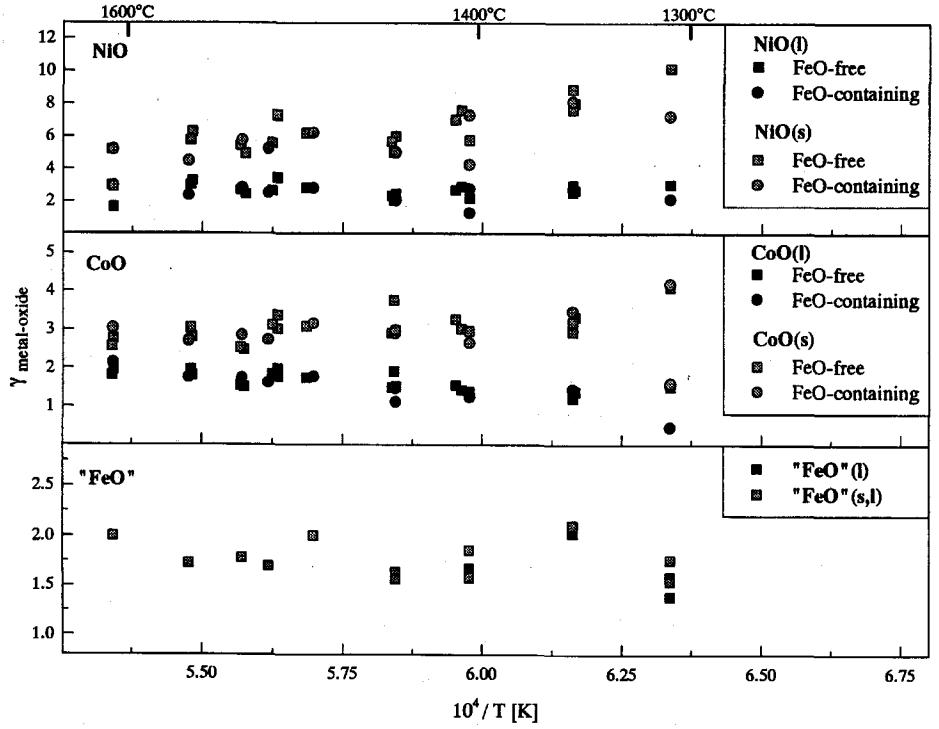

Fig. 5. Activity coefficients vs. temperature. Comparison of solid and liquid standard states of the oxides. Using a solid standard state for NiO produces an increase of γ_{NiO} with temperature. This increase disappears when using the correct liquid standard state. For CoO this results in a slight decrease of γ_{CoO} with temperature.

melts ranging from 0.7 to 2. The FeO activity coefficients for melts with SiO_2 and Al_2O_3 contents similar to those used in the present experiments were about 1.2, somewhat lower than our average of 1.70. The CaO-contents in the liquids used here are a factor of two above those of the melts used by Roeder (1974). The influence of CaO on the FeO activity is unfortunately unknown. It cannot be derived from the data set of Roeder as his samples had rather uniform CaO-contents.

Because $\gamma_{\text{"FeO"}}$ is constant in silicate melts of AD or BK composition within FeO variations from 0 to 12 wt.% and MgO variations from 5 to 20 wt.% MgO, more complicated models, e.g., different choices of mole fractions, are not considered. If we were to consider only the network forming cations for calculating mole fractions, we would obtain the same relative results, except that the absolute numbers would be lower by roughly a factor of two. The increase of $\gamma_{\text{"FeO"}}$ with MgO-contents at high MgO-contents (> 20 wt.%) may indicate the limits of this approach.

A number of studies have attempted to model the NiO activities in silicate melts. Most authors, including a study from this laboratory, have used solid standard states for NiO which leads to very different and strongly temperature-dependent activity coefficients as shown before. Doyle and Naldrett (1987) have determined NiO activities in FeO-free silicate melts at a single oxygen fugacity and a temperature of 1400°C. The activity coefficients of NiO in these melts calculated relative to the NiO liquid standard state are found to be 2.44 ± 0.24, in reasonable agreement with our activity coefficient of 2.70 (Table 4). Activity coefficients were calculated from the Doyle and Naldrett data following the same procedure as above, i.e., relative to NiO(l). As the only major variable in the Doyle and Naldrett (1987) data set is the MgO-content, these data also show that the NiO activity coefficient is independent of the MgO-

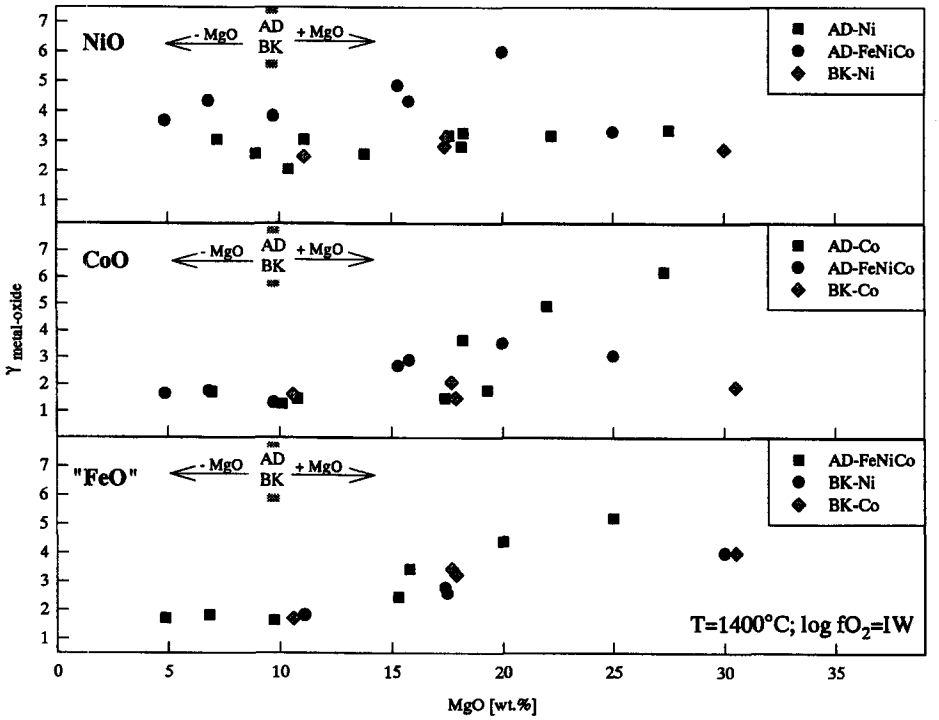

Fig. 6. The effect of addition and removal of MgO to the anorthite–diopside and komatiitic basalt starting compositions on the activity coefficients of NiO, CoO and FeO. There is no dependence up to about 20 wt.% MgO. The important finding is supported by earlier data of Doyle and Naldrett (1987) and by data in Ertel et al. (1996a). At MgO-contents above 20 wt.% there is a small increase in γ_{CoO} and in γ_{FeO}.

content of the silicate liquid, from 0 to 15.5 wt.% MgO, in agreement with findings of this study.

Dingwell et al. (1994) studied the solubility of Ni in melts of anorthite–diopside composition. Their results are in excellent agreement with the results compiled in this study as discussed in Holzheid et al. (1994) and Dingwell et al. (1994). Ertel et al. (1996a) amplified these studies by varying the silicate composition through addition of forsterite. They find constant solubilities up to 16 wt.% MgO in the melt, in agreement with data reported here. In addition, Ertel et al. (1996a) showed that addition of up to 35 wt.% of SiO_2 to the anorthite–diopside eutectic composition does not change the solubility of Ni. Ertel et al. (1996a) also reported a comparatively strong dependence of Ni-solubilities on Ca and on Na. CaO-contents of the liquids studied here were constant and Na-contents were low or even absent.

The independence of γ_{NiO} on the MgO-content of the melt does not contradict the dependence of the Ni olivine/melt partition coefficient $D^{Ni}_{ol/melt}$ on MgO as shown by Hart and Davis (1978). If $D^{Ni}_{ol/melt}$ is derived from the exchange reaction of NiO + Mg-Ol = MgO + Ni-Ol one obtains a relationship of the form $D^{Ni}_{ol/melt} = K \cdot (X_{Mg-Ol}/a_{MgO})$, where K is a constant and it is assumed that Ni-olivine and Mg-olivine mix ideally (Campbell and Roeder, 1968; Seifert and O'Neill, 1987). The mole fraction $X_{Mg\text{-}Ol}$ will be more or less constant as long as forsterite-rich olivine is precipitating from the melt. Thus the $D^{Ni}_{ol/melt}$ is proportional to the activity of MgO in the melt. This will transform into a dependence on the mole fraction of MgO.

Snyder and Carmichael (1992) determined FeO and NiO activities in silicate melts of similar compositions used in this study. Their activity coefficients for FeO (relative to a solid wüstite standard state) vary between 2 and 5.1 and are thus significantly higher than those found in this study and in related work. The NiO-activity coefficients calculated relative to solid NiO range from 8.7 to 33. Recalculations to the liquid standard states yield values from 2.5 to 7, with the majority of data above 3. The reason for this discrepancy is not clear. The Snyder and Carmichael (1992) experiments were done at lower temperatures than our experiments or those of Doyle and Naldrett. Incomplete equilibration of silicates with metal would produce higher activity coefficients. Alternatively, there may be a strong temperature dependence of activity coefficients, but such a dependence was not detected within the temperature range studied in this work.

4.3. Fractionation of Ni / Co ratios by olivine crystallization

The NiO, CoO and FeO activity coefficients in silicate melts (relative to liquid-oxide standard states) obtained in this study show no variation with oxygen fugacity, temperature and to a limited extent with composition. They may therefore be useful in predicting the effect of crystallization of olivine on the Ni/Co ratio in the residual melt. However, we emphasize that this statement is only true for the systems studied here. We have essentially no variation in Al_2O_3 and in CaO in our samples, we have also not included minor elements (e.g., Na, Mn etc.).

It has been known for some time that Ni-olivine mixes more or less ideally with forsterite (Campbell and Roeder, 1968; Seifert and O'Neill, 1987). Deviations from ideal mixing are also small for Co-olivine and forsterite as shown by Seifert and O'Neill (1987). The excess energies of mixing of Ni, Co, Fe and Mg-olivine are so small that activity coefficients derived from them are unity within error limits. For example, from the data of Seifert and O'Neill (1987) it can be shown that for a mixture of $MgSi_{0.5}O_2$ and $NiSi_{0.5}O_2$, $\gamma_{NiSi_{0.5}O_2}$ is unity within the limits of error. It thus appears impossible to explain the observed preferred partitioning of NiO compared to CoO into olivine (e.g., Ehlers et al., 1992) by crystal chemical effects. The comparatively high activity coefficient of NiO in silicate melts offers another explanation for the higher Ni olivine/melt partition coefficient $D^{Ni}_{ol/melt}$. It is a property of the liquid silicate, i.e., the high γ_{NiO}, that is responsible for the preferred partitioning of Ni into olivine. This would imply that the high crystal field stabilization energy (CFSE) of Ni in olivine which is generally assumed to be responsible for the high $D^{Ni}_{ol/melt}$ has no or only a negligible effect on Ni partitioning between olivine and melt (see below).

The constant activity coefficients for NiO, CoO and FeO obtained in this study allow us to quantify the partitioning of Ni and Co between olivine and melt.

Subtraction of the two following equations from each other

$$2NiO(s) + SiO_2(s) = Ni_2SiO_4(s) \quad (10)$$

$$2CoO(s) + SiO_2(s) = Co_2SiO_4(s) \quad (11)$$

then subtraction of NiO(s) = NiO(l) and addition of CoO(s) = CoO(l) leads to:

$$NiO(l) + CoSi_{0.5}O_2(s) = CoO(l) + NiSi_{0.5}O_2(s) \quad (12)$$

From this equation the following relationship may be deduced:

$$\log(X_{NiSi_{0.5}O_2}/X_{CoSi_{0.5}O_2}) = \log(X_{NiO}/X_{CoO}) + \log(\gamma_{NiO}/\gamma_{CoO}) + \log K \quad (13)$$

The first term on the LHS is the molar ratio of Ni- to Co-olivine. The activity coefficients for olivine were assumed to be unity considering the nearly ideal solid solution of Ni-, Co-, Mg- and Fe-olivine. The first term on the RHS is the molar ratio of NiO to CoO and the second term the corresponding activity coefficient ratio.

The calculation of the equilibrium constant K of Eq. (12) is based on recent determinations of the free energy of formation of Ni_2SiO_4 and Co_2SiO_4 from the oxides (Eqs. (10) and (11)) by O'Neill (1987). With additional data from Barin (1989) on NiO and CoO, as discussed before, the following expression for the equilibrium constant of Eq. (12) is derived:

$$\log K(12) = 139.337/T - 2.64 + 0.324\ln T \quad (14)$$

The final expression for the partitioning of Ni/Co between olivine and melt is then:

$$K_D^{Ni/Co} = (X_{NiSi_{0.5}O_2}/X_{CoSi_{0.5}O_2})/(X_{NiO}/X_{CoO}) = (\gamma_{NiO}/\gamma_{CoO}) \cdot K \quad (15)$$

Using an average activity coefficient ratio $\gamma_{NiO}/\gamma_{CoO} = 1.78 \pm 0.44$ (Table 4) the Ni/Co olivine/melt distribution coefficient (K_D) is obtained as:

$$K_D^{Ni/Co} = (Ni/Co)^{Ol}/(Ni/Co)^{melt} = 1.78 \cdot K \quad (16)$$

with K as defined in Eq. (14).

This yields a $K_D^{Ni/Co}$ of 1.13 at 1100°C, 1.21 at 1300°C and 1.34 at 1600°C and is thus only moderately dependent on temperature.

Ehlers et al. (1992) determined ol/melt partition coefficients for NiO and CoO. An average of 14 experiments with MgO-contents between 14 wt.% and 22 wt.% gave a $D_{ol/melt}^{Nio}$ of 5.33 ± 1.57. The average $D_{ol/melt}^{Co}$ of 8 experiments is 2.53 ± 0.42 (6 experiments). This yields a $K_D^{Ni/Co}$ of 2.10 ± 0.71. The $K_D^{Ni/Co}$ at 1350°C calculated here is 1.23 ± 0.31. Although this is considerably below the value of Ehlers et al. (1992) it is still within the combined error limits. In addition, there are some uncertainties in the application of the calculated $K_D^{Ni/Co}$ to the Ehlers et al. data set. Firstly, there is still an incomplete knowledge of the Ni and Co activity coefficients in the alloys used in the experiments, primarily in the ternary alloys. Secondly, there is a large difference in CaO between the melts studied here and the melt compositions used by Ehlers et al.. The magnitude and influence of CaO on the activity coefficients of NiO and CoO is not yet clear. Improving the alloy data basis and given a better understanding of the role of CaO, and also of Na_2O, with regard to NiO and CoO activities, will allow more precise predictions of the Ni/Co-trends produced by olivine fractionation.

4.4. Structural interpretation of activity coefficients

It is interesting to see whether the current state of knowledge of the structure of silicate melts can help to understand the nature and extent of non-ideality of mixing of the Ni-, Co- and Fe-bearing components in the silicate melts. The non-ideality of mixing is a measure of the tendency of a component to remain in solution relative to the ideally diluted standard state. It is instructive to analyze the problem with regard to the component showing the highest degree of non-ideality, NiO. Consideration of the local structure around Ni in these melts provides some rationale for the nature of observed non-ideality. In the solid oxide Ni is present in an octahedral co-ordination; even in quenched glasses a larger proportion of all divalent transition metal cations excepting Co are in an octahedral/distorted octahedral/5-fold coordination (e.g., Keppler, 1992; Brown et al., 1995 etc.).

However, in-situ X-ray and spectroscopic studies show that Ni, and probably the other cations as well, tend to attain a tetrahedral coordination in high-temperature silicate liquids (e.g., Farges and Brown, 1996; Keppler and Bagdassarov, 1996). This suggests that in going to these high-temperature silicate liquids from octahedrally coordinated states in oxides, silicates such as olivines or glasses to the tetrahedral coordination in silicate liquids transition metal cations must lose a part of their ligand-field stabilization energies. This explains the positive deviation from ideality (indicating a preference of the ideally diluted octahedrally coordinated standard state relative to the silicate liquid) and compatible behaviour of these elements during igneous fractionation (preference of the octahedral coordination and the corresponding energetic gain in the crystals relative to the liquids).

A measure of the loss in ligand-field stabilization energy in going from octahedral to tetrahedral coordination is given by the so-called octahedral site preference energy (OSPE; defined as CFSE in octahedral coordination, CFSE in tetrahedral coordination; see Burns, 1985 for more details). Keppler (1992) has estimated the OSPE in albite–diopside melts for Ni^{2+}, Co^{2+} and Fe^{2+} to be 60.0, 29.0 and 11.0 kJ/mol, respectively. It is interesting to note that Ni, with the highest OSPE, is also a constituent of the component (e.g., NiO) which shows the largest positive deviation from ideality in the melt. This indicates that at least for elements which have a high stabilization energy in the octahedral environment, such as Ni, OSPE may play an important role in determining the extent and nature of non-ideality. However, the OSPE alone cannot account quantitatively for the magnitude of the non-ideality. For example, additional contributions to the positive non-ideality may come from the clustering tendency of Ni in silicate melts even when present in small amounts, as found in high-temperature in-situ X-ray studies (Farges and Brown, 1996).

As a change of coordination is a physical process occurring within the liquid itself, it implies that consideration of crystal chemistry alone or a different choice of liquid components cannot be adequate, in all cases, to account for the partitioning behaviour of elements between crystalline phases, e.g. olivine and silicate melts. Indeed, as discussed above, the fractionation of Ni and Co during partitioning between olivine and melt can be largely attributed to the relatively unfavourable tetrahedral sites which Ni is apparently required to occupy in high-temperature liquids. A further indication that OSPE may play a role in determining the partitioning behaviour is obtained from the study of Beattie (1994), who measured olivine–liquid partition coefficients for a number of transition metal and non-transition metal elements. While all partition coefficients for divalent non-transition metal cations are described by a "strain-compensated curve" (e.g., Beattie, 1994; Blundy and Wood, 1994), data for all transition metal cations excepting Mn fall away from the curve. The fact that Mn^{2+} is the only transition metal cation without any crystal field stabilization energy indicates that the reason for the mismatch may be the inability of the strain-compensated curve to account for the stabilizing effects of crystal field splitting. However, further quantification is difficult because the stabilizing effects of crystal field splitting exist in solids as well as short-range ordered liquids such as silicate melts. Therefore, in the general case it is necessary to measure and evaluate the relative roles of crystal field splitting stabilization energies in both phases before the overall effect on element partitioning may be calculated. In the specific case of Ni partitioning between olivine and melt discussed above, the non-ideality in the liquid phase was found to play the determining role as the Ni-, Co-olivines show nearly ideal behaviour overall, in spite of the obvious presence of crystal field stabilization, lattice strain, ordering and other factors which should contribute to non-ideality. This highlights the fact that the energetics of mixing in silicates is complex and determined by a number of factors which may compensate each other to some extent and sometimes even lead to mutual cancellation and a fortuitous overall ideal or near-ideal behaviour (e.g., see Ganguly and Saxena, 1987, for a detailed discussion).

The fact that the local environment of Ni ions in high-temperature liquids and quenched glasses have been found to be different has two interesting implications in the context of activities and element partitioning: (a) for evaluating the role of CFSE/OSPE in high T magmatic systems, data from in-situ high-temperature measurements in liquids are necessary, and (b) although not observed over the temperature

range of this study, the activity coefficients and hence the partitioning of Ni between olivine and silicate melt must show a change in temperature dependence at some point as the structural location of Ni changes from dominantly tetrahedral to dominantly 5- or 6-coordinated at some lower temperature, which is the state found frozen in the glasses studied. In fact, it can be speculated that with increasing temperature there are two competing processes at work—a change of coordination from dominantly 5- or 6-fold in crystals and glasses to 4-fold in the liquids (tending to increase deviation from ideality according to the above analysis) and the usual increase in configurational entropy (tending to make the system more ideal), such that over the temperature range of measurement the effects fortuitously balance each other and lead to more or less temperature-independent activity coefficients.

Acknowledgements

This research was, in part, supported by the Deutsche Forschungsgemeinschaft (DFG). Comments by J. Ganguly, H.St.C. O'Neill and P. Hess are appreciated.

References

Barin, I., 1989. Thermochemical Data of Pure Substances. VCH, Weinheim, Basel, Cambridge.

Beattie, P., 1994. Systematics and energetics of trace-element partitioning between olivine and silicate melts: implications for the nature of mineral/melt partitioning. Chem. Geol. 117, 57–71.

Blundy, J., Wood, B.J., 1994. Prediction of crystal-melt partition coefficients from elastic moduli. Nature 372, 452–454.

Borisov, A., Palme, H., 1995. The solubility of iridium in silicate melts: new data from experiments with $Ir_{10}Pt_{90}$ alloys. Geochim. Cosmochim. Acta 59, 481–485.

Borisov, A., Palme, H., Spettel, B., 1994. Solubility of palladium in silicate melts: implications for core formation in the Earth. Geochim. Cosmochim. Acta 58, 705–716.

Brown, G.E. Jr., Farges, F., Calas, G., 1995. X-ray scattering and X-ray spectroscopy studies of silicate melts, in structure, dynamics and properties of silicate melts. In: J.F. Stebbins, P.F. McMillan and D.B. Dingwell (Editors), Reviews in Mineralogy, Vol. 32. Mineralogical Society of America, Washington, DC, pp. 277–316.

Burns, R.G., 1985. Thermodynamic data from crystal field spectra, in microscopic to macroscopic—atomic environments to mineral thermodynamics. In: S.W. Kieffer and A. Navrotsky (Editors), Reviews in Mineralogy, Vol. 14. Mineralogical Society of America, Washington, DC.

Campbell, I.H., Roeder, P.L., 1968. The stability of olivine and pyroxene in the Ni–Mg–Si–O system. Am. Mineral. 53, 257–268.

Campbell, I.H., Naldrett, A.J., Roeder, P.L., 1979. Nickel activity in silicate liquids: some preliminary results. Can. Mineral. 17, 495–505.

Colson, R.O., 1992. Solubility of neutral nickel in silicate melts and implication for the Earth's siderophile element budget. Letters to Nature. Nature 357, 65–68.

Dingwell, D.B., O'Neill, H.St.C., Ertel, W., Spettel, B., 1994. The solubility and oxidation state of Ni in silicate melt at low oxygen fugacity: results using a mechanically assisted equilibrium technique. Geochim. Cosmochim. Acta 58, 1967–1974.

Doyle, C.D., Naldrett, A.J., 1987. Ideal mixing of divalent cations in mafic magma, II. The solution of NiO and the partitioning of nickel between coexisting olivine and liquid. Geochim. Cosmochim. Acta 51, 213–219.

Ehlers, K., Grove, T.L., Sisson, T.W., Recca, S.I., Zervas, D.A., 1992. The effect of oxygen fugacity on the partitioning of nickel and cobalt between olivine, silicate melt, and metal. Geochim. Cosmochim. Acta 56, 3733–3743.

Ertel, W., Dingwell, D.B., O'Neill, H.St.C., 1996a. Composition dependence of the activity of Ni in silicate melts. Geochim. Cosmochim. Acta (submitted).

Ertel, W., O'Neill, H.St.C., Dingwell, D.B., Spettel, B., 1996b. Solubility of tungsten in a haplobasaltic melt as function of temperature and oxygen fugacity. Geochim. Cosmochim. Acta 60, 1171–1180.

Farges, F., Brown, G.E. Jr., 1996. An empirical model for the anharmonic analysis of high-temperature XAFS spectra of oxide compounds with applications to the coordination environment of Ni in NiO, Ni_2SiO_4 and Ni-bearing Na-disilicate glass and melt. Chem. Geol. 128, 93–106.

Ganguly, J., Saxena, S.K., 1987. Mixtures and Mineral Reactions. Springer-Verlag, Berlin, 291 pp.

Hart, S.R., Davis, K.E., 1978. Nickel partitioning between olivine and silicate melt. Earth Planet. Sci. Lett. 40, 203–219.

Holzheid, A., Palme, H., 1996a. The influence of FeO on the solubility of Co and Ni in silicate melts. Geochim. Cosmochim. Acta 60, 1181–1193.

Holzheid, A., Palme, H., 1996b. Accretion and early history of the Earth: constraints imposed by Ni and Co abundances in the Earth's mantle. In: Lunar Planet. Sci. XXVII. Lunar Planet. Inst., Houston, TX, pp. 559–560.

Holzheid, A., Borisov, A., Palme, H., 1994. The effect of oxygen fugacity and temperature on solubilities of nickel, cobalt, and molybdenum in silicate melts. Geochim. Cosmochim. Acta 58, 1975–1981.

Keppler, H., 1992. Crystal field spectra and geochemistry of transition metal ions in silicate melts and glasses. Am. Mineral. 77, 62–75.

Keppler, H., Bagdassarov, N., 1996. High-temperature electronic absorption spectra of Co^{2+} and Ni^{2+} in silicate glasses and melts to 1500°C. In: EMPG VI, Bayreuth. Terra Abstr., p. 32.

Leeman, W., Lindstrom, D.J., 1978. Partitioning of Ni^{2+} between basaltic and synthetic melts and olivines—an experimental study. Geochim. Cosmochim. Acta 58, 801–816.

O'Neill, H.St.C., Pownceby, M.I., 1993. Thermodynamic data from redox reactions at high temperatures, I. An experimental and theoretical assessment of the electrochemical method using stabilized zirconia electrolytes, with revised values for the Fe-"FeO", Co-CoO, Ni-NiO and Cu-Cu_2O oxygen buffers, and new data for the W-WO_2 buffer. Contrib. Mineral. Petrol. 114, 296–314.

O'Neill, H.St.C., 1987. Free energies of formation of NiO, CoO, Ni_2SiO_4 and Co_2SiO_4. Am. Mineral. 72, 280–291.

O'Neill, H.St.C., Dingwell, D.B., Borisov, A., Spettel, B., Palme, H., 1995. Experimental petrochemistry of some highly siderophile elements at high temperatures, and some implications for core formation and the mantle's early history. Chem. Geol. 120, 255–273.

Righter, K., Drake, M.J., Yaxley, G., 1996. Prediction of siderophile element metal/silicate partition coefficients to 20 GPa and 2800°C: the effects of pressure, temperature, oxygen fugacity, and silicate and metallic melt composition. Phys. Earth Planet. Inter. (submitted).

Roeder, P.L., 1974. Activity of iron and olivine solubility in basaltic liquids. Earth Planet. Sci. Lett. 23, 397–410.

Schmitt, W., Palme, H., Wänke, H., 1989. Experimental determination of metal/silicate partition coefficients for P, Co, Ni, Cu, Ga, Ge, Mo, and W and some implications for the early evolution of the Earth. Geochim. Cosmochim. Acta 53, 173–185.

Seifert, S. and O'Neill, H.St.C., 1987. Experimental determination of activity–composition relations in Ni_2SiO_4–Mg_2SiO_4 and Co_2SiO_4–Mg_2SiO_4 olivine solid solutions at 1200 K and 0.1 MPa and 1573 K and 0.5 GPa. Geochim. Cosmochim. Acta 51, 97–104.

Snyder, D.A., Carmichael, S.E., 1992. Olivine–liquid equilibria and the chemical activities of FeO, NiO, Fe_2O_3, and MgO in natural basic melts. Geochim. Cosmochim. Acta 56, 303–318.